J. At. Mol. Sci.
doi: 10.4208/jams.111009.120609a

Vol. **1**, No. 1, pp. 78-86
February 2010

Structural stability and electronic structure of N- or C-monodoped TiO_2 from first-principles calculations

Chao-Hua Ma, Xin-Guo Ma*, Cheng-Guo Li, and Ling Miao

Department of Electronic Science and Technology, Huazhong University of Science and Technology, Wuhan 430074, China

Received 10 November 2009; Accepted (in revised version) 6 December 2009;
Available online 15 February 2010

Abstract. Plane-wave ultrasoft pseudopotential calculations are performed to study the structural stability and the electronic structure of N- or C-monodoped TiO_2. Firstly, various models of nonmetal doped TiO_2 are optimized to calculate the defect formation energy of different dopants. It is found that the Ti-rich condition facilitates N- or C-doping. The nonmetallic oxide of C and N in high valence facilitates doping under the Ti-rich condition. The element and the oxide of C and N in low valence facilitate doping under the O-rich condition. Secondly, the energy band structure of doped TiO_2 is analyzed. The results show that N-doping generates a semi-filled shallow impurity energy level near the top of the valence band. C-doping generates three deep impurity energy levels within the band gap which easily become the recombination centers of electrons and holes. Finally, the bonds between atoms are analyzed using the electron density map and the bond population. It is found that the electronegativity of impurities determines the position of the impurity energy level. These results help to understand the effects of nonmetal doping on the photocatalytic properties of TiO_2.

PACS: 78.20.-e, 71.55.-i, 71.15.Mb

Key words: photocatalysis, stability, first-principles, TiO_2

1 Introduction

TiO_2 is a promising semiconductor material with wide band gap which presents excellent photoelectric and photocatalytic properties. It has received intense attention in the photocatalytic technology [1,2] and dye sensitized solar cells [3,4]. However, the wide band gap (3.23 eV) and high photo-generated electron-hole recombining rate limit its application in the photocatalytic field. So it is necessary to perform modification. A common modifying method is transition metal doping, such as V-, Cr-, Mn-, Fe-, Co- and Nb-doping [5, 6].

*Corresponding author. *Email address:* maxg2008@yahoo.cn (X. G. Ma)

The photocatalytic activity of transition metal cation doped TiO_2 is decreased except for few cases, since these doping methods generate deep local level of dopant which easily becomes recombination center of electrons and holes [5–7]. However, nonmetal doped TiO_2 is the photocatalytic material with excellent performance. For example, sputtering has been used to prepare $TiO_{2-x}N_x$ coating by Asahi *et al*. [8]. It is found that the electronic states of N $2p$ orbital narrow the band gap by mixing those of O $2p$ orbits. Also, the spectral response clearly moved to the visible region. The experimental results show that N-, C- and other nonmetal doping help to improve the photocatalytic performance [9]. It is also found that the impurity energy levels of nonmetal doped TiO_2 are likely to form the recombination centers of electrons and holes, which reduce the photocatalytic efficiency [10, 11].

The preparation methods and conditions of these photocatalyst materials are different, which leads to the difference of the geometry structure and the material composition. It is very difficult to analyze the modification mechanism of nonmetal doped TiO_2 using experiment. Thus, it is necessary to study the stability of geometry structure and energy band structure using first-principle method [12]. Valentin *et al*. [13] have used ultrasoft pseudopotential method to study the electronic structure and the defect formation energies of C-doped TiO_2. But they have not considered the charged defect formation energies. Recently, the C- or N-doped TiO_2 have been studied by Yang *et al*. [14] and Tao *et al*. [15] and have been found to have ferromagnetism. However, the type and stability of the doped structure have not been studied. Many studies have shown that nonmetal doped TiO_2 can effectively enhance the range of spectral response [16–19]. High concentrations of nonmetal doping are difficult to achieve, which restricts its application in the photocatalytic fields. Thus, first-principles calculations are performed to study nonmetal doped TiO_2. Then the defect formation energies are calculated. After that, the effects of doping species on the impurity concentration are discussed. Finally, the electronic structure and the electrical charge population are analyzed.

2 Computational methods

Plane-wave ultrasoft pseudopotential method based on the density functional theory is used in the calculations. The configurations of valence electrons are selected as C: $2s^2 2p^2$, N: $2s^2 2p^3$, O: $2s^2 2p^4$ and Ti: $3s^2 3p^6 3d^2 4s^2$ when describing the ion solid interaction with the valence electrons. The other orbital electrons are calculated as core electrons. The PW91 generalized gradient approximation formulism for the exchange and correlation function is chosen [20] in the calculations of anatase TiO_2. According to the reference [21], geometry parameters of TiO_2 calculated by PBE [22] formulism and RPBE [23] formulism are closer to the experimental values [24]. The Pulay density mixing method is used in the computations of self-consistent field. The self-consistent accuracy is set to the degree that every atomic energy converges to 2.0×10^{-6} eV and the force on every atom is smaller than 0.1 eV/nm. The BFGS algorithm is used in the structural optimization of the

model, and every atomic energy converges to 2.0×10^{-5} eV. First Brillouin zone is divided into $5\times5\times3$ k-point mesh. The cutoff energy is selected as 380 eV. All the calculations is completed using CASTEP [25] software.

A structure of $2\times2\times1$ supercell containing 48 atoms is established during calculation. Three types of models in which N and C impurities replace O, Ti and the lattice interstitial site are mainly considered for nonmetal doped TiO_2. The structures of six models are built, as shown in Fig. 1. A variety of compounds of N and C are incorporated to explore the preparation conditions and stability of geometry structure when the chemical potentials of N and C impurities are taken into consideration. The gas molecules are put into a cubic lattice of 1 nm^3 to calculate the total energy of N_2 (g), NO (g) and NO_2 (g). The optimized bond lengths are 0.1119 nm, 0.1166 nm and 0.1203 nm, respectively. The error of the result compared with other theoretical calculations is less than 2% [26]. Similarly, CO (g) and CO_2 (g) are calculated. The layered crystal structure of graphite is selected to calculate the total energy for C element.

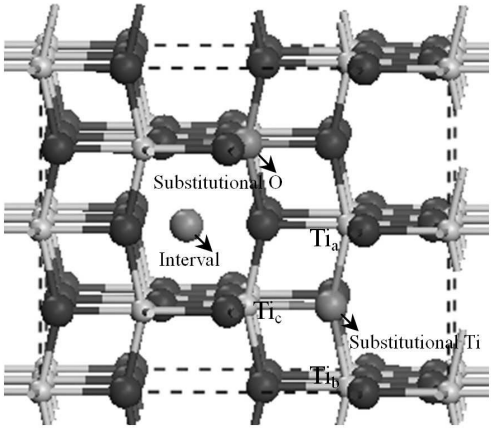

Figure 1: The structure of $2\times2\times1$ supercell of nonmetal-doped TiO_2. The small grey spheres, the black spheres and the big grey spheres represent Ti atoms, O atoms and non-metallic impurity atoms, respectively.

3 Results and discussion

3.1 Defect formation energy

The effect of different impurity atoms varies with the geometric structure of TiO_2 when the model of nonmetal doped TiO_2 is optimized. The stability of the doped system also changes a lot. The defect formation energy of nonmetal doped TiO_2 is calculated to compare the model structural stability of the doped TiO_2 and the concentration of dopants. For a defect with a charge q, its formation energy is expressed as

$$E_f = E_T(doped) - E_T(undoped) + n_{NM}\mu_{NM} + n_{Ti}\mu_{Ti} + n_O\mu_O + q(E_F + E^q_{VBM}). \quad (1)$$

Here E_T (doped) is the total energy of the system containing the non-metallic impurity; E_T (undoped) is the total energy of the pure system; n_{Ti} and n_O are the number of Ti and O atoms removed; n_{NM} is the number of non-metallic impurity atoms added; μ_{NM}, μ_{Ti} and μ_O are the chemical potentials of non-metallic impurity atoms, Ti and O, respectively; E_f is the Fermi energy measured from the valence-band maximum (VBM). The chemical potentials depend on the experimental growth conditions, which can be Ti-rich or O-rich (or anything in between). The effect of different impurities in the neutral charge defects on formation energy is summarized in Tables 1 and 2. C impurities are selected as graphite, gaseous CO and gaseous CO_2, in which the valence of C element are 0, -2, and -4. The N impurities are in the forms of gaseous N_2, NO and NO_2, in which the valence of N element are 0, -2, and -4.

Table 1: The defect formation energy (in eV) of monodoped TiO_2 with different impurity of C under various growth conditions.

Types of defects	Growth condition	C	CO	CO_2
C_O	O-rich extreme	9. 02	9. 93	13. 51
	Ti-rich extreme	3. 87	-0. 37	-1. 94
C_{Ti}	O-rich extreme	-1. 24	-0. 34	3. 24
	Ti-rich extreme	9. 06	4. 81	3. 24
C_i	O-rich extreme	5. 58	6. 49	10. 07
	Ti-rich extreme	5. 58	1. 34	-0. 23

Table 2: The defect formation energy (in eV) of monodoped TiO_2 with different impurity of N under various growth conditions.

Types of defects	Growth condition	N_2	NO	NO_2
N_O	O-rich extreme	5. 18	4. 83	5. 95
	Ti-rich extreme	0. 03	-5. 47	-9. 50
N_{Ti}	O-rich extreme	1. 89	1. 54	2. 66
	Ti-rich extreme	11. 69	6. 69	2. 66
N_i	O-rich extreme	5. 72	5. 37	6. 49
	Ti-rich extreme	5. 72	0. 22	-3. 81

Under O-rich condition, there are C_{Ti} defects with low defect formation energy in the three reactants, of which the formation energy of doped TiO_2 using graphite as dopant source is the lowest, which is -1.24 eV, as shown in Tables 1 and 2. It means that the concentration of C_{Ti} in doped TiO_2 using graphite as dopant source is high under O-rich condition. There are low formation energies of C_O defect in the three reactants under Ti-rich condition, of which the defect formation energy of doped TiO_2 using CO_2 as dopant source is the lowest, which is -1.94 eV. This means that Ti-rich condition is beneficial for the replacement of O atom by C atom. N_{Ti} defect under O-rich condition has low defect formation energy with three kinds of impurity reactants for a variety of defects formed by N-doping, of which the formation energy of doped TiO_2 using NO as dopant source is the

lowest, which is 1.54 eV. However, this formation energy of defects is significantly higher than that in C_{Ti} situation. The cause may be that the electronegativity of N is greater than that of C and is closer to that of O. The formation energy of N_O defect is the lowest among the three kinds of impurity under Ti-rich condition, of which the formation energy of doped TiO_2 using NO or NO_2 as dopant source is negative. In summary, nonmetallic elemental oxides in high valence contribute to doping under Ti-rich condition; elements and oxide with low valence contribute to doping under O-rich condition.

It is important that accurate calculations and analysis of the influence of charged point defects on the defect formation energy. According to a recent experimental study, N and C will replace O in the lattice easily after annealing, because the electronegativity of N and C is similar to that of O. The impurity atoms form bonds with the surrounding Ti atoms after nonmetal-doping. Impurity energy levels are generated in the valence band (VBM) or above the top of the VB in the band gap. The charge states of the defect model replaced by N and Ti are calculated and analyzed, as shown in Fig. 2. There is a changed energy level at the top of VBM. It is ε_{C_O} (+1/-2) =E_{VBM}+1.08 eV in triplet state after O is replaced by C. It means that a few deep impurity energy levels emerge near the changed energy level. There is also a changed energy level at the top of VBM. It is ε_{N_O} (0/-1) =E_{VBM}+0.26 eV in single state after O is replaced by C. It means that a shallow impurity energy level emerges near the changed energy level.

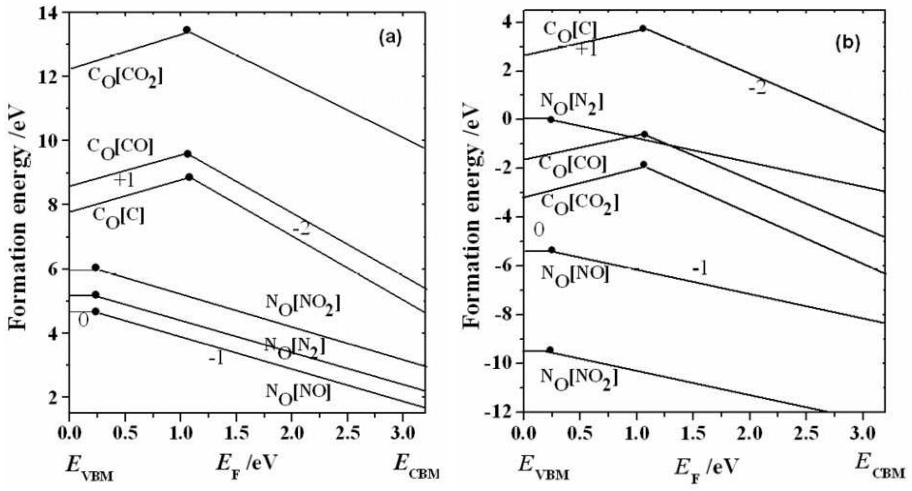

Figure 2: The function between the formation energy of the charge defects and the Fermi level of anatase TiO_2, solid points represent the positions of thermodynamically changed energy level $\varepsilon(q_1/q_2)$: (a) O-rich condition, (b) Ti-rich condition.

3.2 Electronic structure

The electronic structure is calculated to further analyze the effect of O position replaced by nonmetal in TiO_2 on the physical and chemical properties. Fig. 3 (a) shows the appear-

ance of three defect energy levels in the band gap after O is replaced by C. The distances from them to the original O 2*p* state are between 0.8 eV and 1.7 eV. Deep acceptor defect energy levels emerge, all of which are provided by C 2*p* state. The figure shows that the middle defect energy level is just filled up by electrons when the defect state is neutral. In this case, the band gap of TiO_2 in local position of defects is reduced by about 1 eV. The reduction of band gap is beneficial for the visible light absorption, extending the region of the absorption spectrum of the sunlight. However, there is an empty defect energy level about 0.7 eV above the Fermi level, which easily becomes the recombination center of photo-generated electrons and holes. Ti 3*d* energy level has moved a little which reduces the band gap to 2.11 eV after N-doping, as shown in Fig. 3 (b). This is due to the asymmetric strengthening of the crystal field around Ti, in other words, TiO_6 octahedron is distorted. There are two explanations. On one hand, N atom has one less outer electron than O atom and the potential of N 2*p* states is slightly higher than that of O 2*p* states. On the other hand, N 2*p* orbital and Ti 3*d* orbital are hybridized. As a result, N 2*p* states split. Part of them move down to VBM and overlap O 2*p* states, of which one energy level shifts to 0.3 eV above the valence band and a defect level is generated above VBM in the band gap. The defect energy level is semi-filled when it is neutral, and easily becomes recombination center of electrons and holes. An electron on donor level passivates a hole on the acceptor level inside the band gap, so the systems still keep semiconductor character, which promotes the separation of electron-hole pairs excited by photo irradiation.

The bond populations between C or N and the surrounding three Ti atoms are positive, which indicates that they are covalent bonds, as shown in Table 3. And such difference of the bond populations indicates that the covalent bond in the direction of c is weaker than the other two bonds. Since electronegativity of N is stronger than that of C,

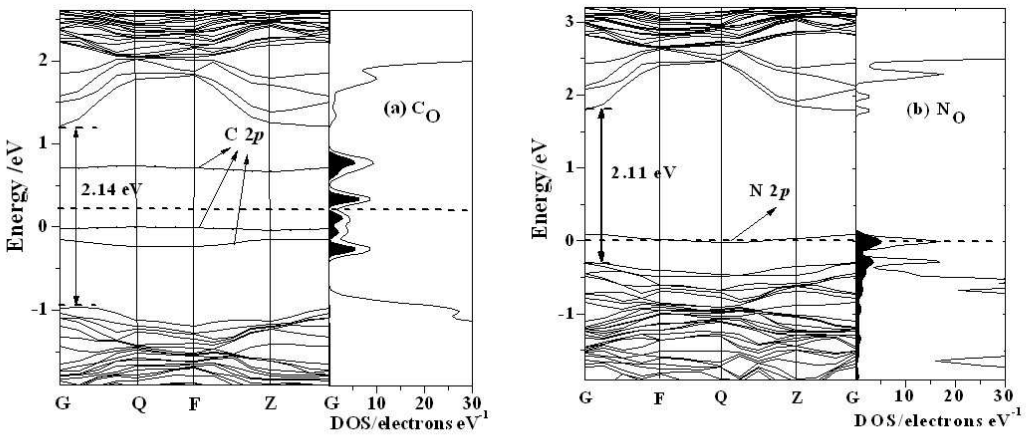

Figure 3: The energy band structure and the density of states in neutral defect states after C and N atoms replacing O atoms in the anatase TiO_2. The dashed line represents the position of the Fermi level.

Table 3: The bond populations between three neighboring Ti atoms and C or N atoms which replace O atoms.

Type of bond	Bond population
C-Ti_a	0.347
C-Ti_b	0.347
C-Ti_c	0.248
N-Ti_a	0.356
N-Ti_b	0.356
N-Ti_c	0.229

the N$-$$Ti_a$ and N$-$$Ti_b$ covalent bonds are stronger than those under C-doped condition. However, the N$-$$Ti_c$ bond is weaker than C$-$$Ti_c$ bond.

Figs. 4 and 5 demonstrate the electron density distribution of the C- and N-monodoped anatase TiO_2 lattice in the planes of "0, 1/2, 0" and "1/2, 0, 0". It can be seen that C or N combine with Ti in the form of covalent bond. As the outermost electron of C and N atoms are two and one less than those of O atoms, respectively, the charge densities around C and N atoms are smaller than that of O atom. The electronegativity of O, N and C are 3.44, 3.04 and 2.55, respectively. It explains the incorporation of C is more likely to generate covalent bond.

4 Conclusion

In summary, the defect formation energy of N- or C-monodoped TiO_2 is affected by the model and the type of doping. To be specific, Ti-rich condition contributes to N- or C-

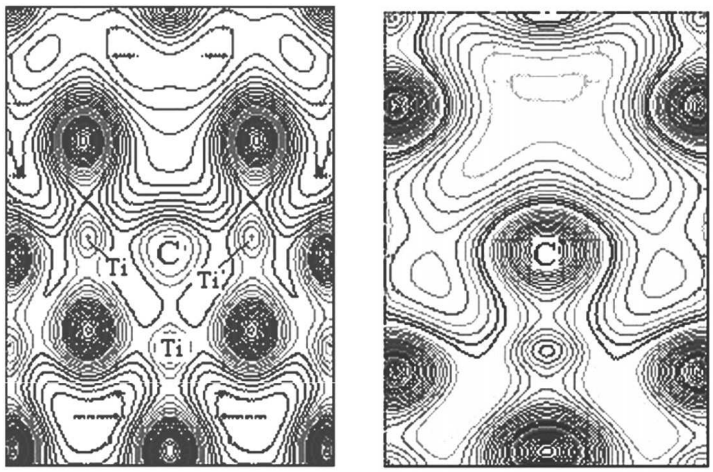

(a) (b)

Figure 4: Electron density distribution map of C anion-doped anatase TiO_2: (a) <0, 1/2, 0> plane, (b) <1/2, 0, 0> plane.

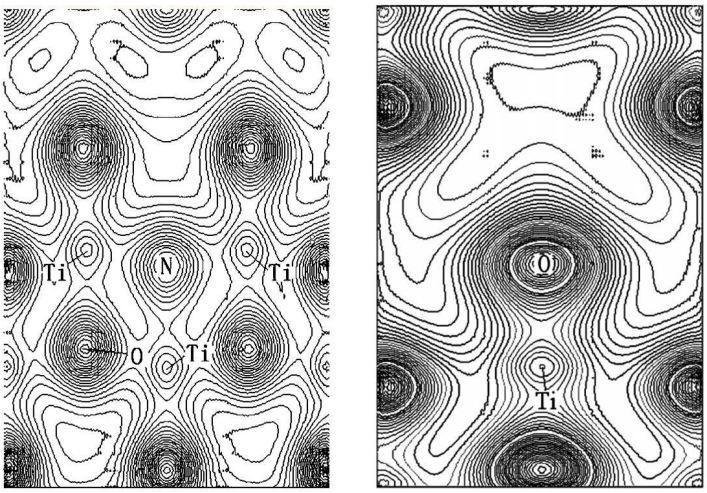

Figure 5: Electron density distribution map of N anion-doped anatase TiO_2: (a) <0, 1/2, 0> plane, (b) <1/2, 0, 0> plane.

doping. The oxide of nonmetallic element for high valence facilitates doping under Ti-rich condition. The element and oxide of low valence facilitate doping under O-rich condition. By comparing the energy band structure of N-monodoped TiO_2 with that of C-monodoped TiO_2, it is found that the latter narrows the band gap, which facilitates the visible light absorption. However, it generates three deep impurity energy levels inside the band gap, which easily become the recombination centers for electrons and holes, thereby reducing the photocatalytic efficiency. The N-doping generated a half-filled impurity energy level near the top of VBM, which also easily forms the recombination centers for electrons and holes, but can be solved by adding an electron. From the electron density map and the bond populations, it is concluded that the location of impurity energy levels is related to the electronegativity of dopants.

References

[1] A. Fujishima and K. Honda, Nature 37 (1972) 238.
[2] F. Zhou and K. M. Liang, Acta Phys. Sin. 54 (2005) 2863 (in Chinese).
[3] S. Y. Huang, G. Schlichthorl, A. J. Nozik, *et al*., J. Phys. Chem. B 101 (1997) 2576.
[4] P. Wang, S. M. Zakeeruddin, J. E. Moser, *et al*., Nature Mater. 2 (2003) 402.
[5] T. Umebayashi, T. Yamaki, H. Itoh, *et al*., J. Phys. Chem. Solids 63 (2002) 1909.
[6] W. Choi, A. Termin, and M. R. Hoffmann, J. Phys. Chem. 98 (1994) 13669.
[7] T. Nishikawa, T. Nakajima, and Y. Shinohara, J. Mol. Struct. (Theochem.) 545 (2001) 67.
[8] R. Asahi, T. Morikawa, T. Ohwaki, *et al*., Science 293 (2001) 269.
[9] S. U. M. Khan, M. Al-Shahry, W. B. Ingler, *et al*., Science 297 (2002) 2243.
[10] T. Okato, T. Sakano, and M. Obara, Phys. Rev. B 72 (2005) 115124.
[11] M. Mrowetz, W. Balcerski, A. J. Colussi, *et al*., J. Phys. Chem. B 108 (2004) 17269.

[12] Y. D. Liu, M. X. Song, L. Bian, *et al*., J. At. Mol. Phys. 25 (2008) 1097 (in Chinese).
[13] C. D. Valentin, G. Pacchioni, and A. Selloni, Chem. Mater. 17 (2005) 6656.
[14] K. S. Yang, Y. Dai, B. B. Huang, *et al*., Appl. Phys. Lett. 93 (2008) 132507.
[15] J. G. Tao, L. X. Guan, J. S. Pan, *et al*., Appl. Phys. Lett. 95 (2009) 062505.
[16] R. Asahi, T. Morikawa, T. Ohwaki, *et al*., Science 293 (2001) 269.
[17] J. Lee, J. Park, and J. Cho, Appl. Phys. Lett. 87 (2005) 011904.
[18] C. D. Valentin, G. Pacchioni, and A. Selloni, Phys. Rev. B 70 (2004) 085116.
[19] Y. Nakano, T. Morikawa, T. Ohwaki, *et al*., Appl. Phys. Lett. 87 (2005) 052111.
[20] J. P. Perdew and Y. Wang, Phys. Rev. B 45 (1992) 13244.
[21] X. G. Ma, J. J. Jiang, and P. Liang, Acta Phys. Sin. 57 (2008) 3120 (in Chinese).
[22] J. P. Perdew, K. Burke, and M. Ernzerhof, Phys. Rev. Lett. 77 (1996) 3865.
[23] B. Hammer, L. B. Hansen, and J. K. Norskov, Phys. Rev. B 59 (1999) 7413.
[24] J. K. Burdett, T. Hughbanks, G. J. Miller, *et al*., J. Am. Chem. Soc. 109 (1987) 3639.
[25] M. D. Segall, Philip J. D. Lindan, M. J. Probert, *et al*., J. Phys.: Condens. Matter 14 (2002) 2717.
[26] X. Z. Zhang, S. H. Chen, and R. M. Jiang, Concise Structural Chemistry (Huazhong University of Science and Technology, Wuhan, 1993).